Journal of Pharmaceutical and Biomedical Analysis 225 (2023) 115219

Contents lists available at ScienceDirect

Journal of Pharmaceutical and Biomedical Analysis

journal homepage: www.journals.elsevier.com/journal-of-pharmaceutical-and-biomedical-analysis

Extrahepatic in vitro metabolism of peptides; comparison of human kidney and intestinal S9 fraction, human plasma and proximal tubule cells, using cyclosporine A, leuprorelin, and cetrorelix as model compounds

Juha Jyrkäs [a,b,*,1], Toni Lassila [a], Ari Tolonen [a]

[a] Admescope Ltd, Typpitie 1, 90620 Oulu, Finland
[b] Research Unit of Sustainable Chemistry, Faculty of Technology, University of Oulu, P.O. Box 3000, 90014 Oulu, Finland

ARTICLE INFO

Keywords:
Extrahepatic peptide metabolism
Metabolite screening
Metabolite identification
Mass Spectrometry
LC/MS

ABSTRACT

Peptide therapeutics showcase number of advantages compared to the traditional small molecule drugs, e,g. they usually have higher affinity to target and lower toxicity profiles. Endogenous peptides are mostly cleared from the body through renal clearance or proteolytic hydrolysis. As a part of drug discovery, metabolite identification is an important part in their development to identify metabolic hot spots and to further improve their stability. As the catabolism of the peptides and peptide-like drugs is often considered to be extrahepatic, the use of in vitro systems derived from these organs might be beneficial. In this study, multiple extrahepatic metabolic systems were evaluated for the applicability for peptide metabolism studies. Three peptide drugs (leuprorelin, cetrorelix, cyclosporin) were incubated in kidney and intestinal S9 fraction (± NADPH), fresh plasma (anticoagulants EDTA and heparin separately), and plated proximal tubule cells. Additionally, leuprorelin was also incubated with human kidney microsomes and cytosol to further investigate the NADPH-dependent metabolism detected in kidney S9 fraction. Both substrate disappearance and metabolite formation were monitored, using UPLC/HR-MS analysis of the collected samples.Overall, the largest number of metabolites was formed in the incubation with kidney S9 fraction, followed by intestinal S9, while incubations with proximal tubule cells produced lower number of metabolites All investigated peptides were stable in plasma and only a few metabolites were detected, likely because the studied peptide drugs have been optimized to be stable in plasma. Leuprorelin showed NADPH-dependent metabolite formation in kidney S9 fraction, while the metabolism of cetrorelix was more NADPH independent. As expected, formation of cytochrome P450 (CYP) catalyzed metabolism of cyclosporine was not observed with the employed extrahepatic systems. The NADPH-dependent metabolism of leuprorelin was detected also in the incubation with kidney cytosol, but not with kidney microsomes, and was thus not caused by CYPs or FMOs, but with cytosolic NADPH-dependent drug metabolizing enzymes. These enzymes could, in principle, activate the amide bond via reductive or oxidative metabolism outside the amide bond. The identity of the involved drug metabolizing enzymes in this process is still unknown.

1. Introduction

Peptide drugs are amino acid chains usually linked together with peptide bonds and are commonly defined as consisting of less than 50 amino acids, which results in maximum 5000 – 6000 Da in molecular weight [1]. Typically, these compounds have a short in vivo half-life, caused by quick degradation into shorter peptides via hydrolysis of amide bonds catalyzed by various proteolytic enzymes [2]. As the metabolism or catabolism of the peptide drugs is rarely based on the reactions catalysed by the cytochrome P450 (CYP)-enzymes, it is beneficial to investigate metabolism in extrahepatic in vitro enzyme sources as a part of the preclinical ADME (absorption, disposition, metabolism, and excretion) – studies.

Peptide drugs are rarely administered orally due to the reasons involving instability in stomach, caused by the acid-catalysed degradation and low permeability through the gastro-intestinal tract [3]. Various solutions to enhance the oral delivery of peptides have been developed over the years [4], and thus the first-pass metabolism should

* Correspondence to: Symeres, Kerkenbos 1013, 6546 BB Nijmegen, Netherlands.
E-mail address: juha.jyrkas@symeres.com (J. Jyrkäs).
[1] current address: Symeres, Kerkenbos 1013, 6546 BB Nijmegen, Netherlands

https://doi.org/10.1016/j.jpba.2022.115219
Received 15 October 2022; Received in revised form 6 December 2022; Accepted 29 December 2022
Available online 31 December 2022

be taken into account when investigating orally administered peptide drugs. The kidneys can rapidly filtrate hydrophilic peptides with molecular weight between 2 and 25 kDa and they are not readily reabsorbed via renal proximal tubule [5]. When peptide drugs are administered subcutaneously or intravenously, the proteolytic enzymes of the plasma are immediately in contact with the peptide drug. Thus, the plasma stability of the peptide drugs is often screened during the pre-clinical ADME–studies [6]. There has been reports of varying plasma stability of therapeutic peptides when different anticoagulants were used, and EDTA has also be shown to be an inhibitor of carboxypeptidases A and B, which might affect the stability [7,8]. In this study, two anticoagulants, EDTA and heparin, were used to evaluate the effect on the stability of the model peptide drugs.

The objective of this study was to investigate three peptide drugs in several extrahepatic human in vitro enzyme sources for their stability and metabolism. The selected peptide drugs were leuprorelin (also known as leuprolide), cetrorelix and cyclosporine, which exhibit different base structures e.g. linear and cyclic, and differences regarding in vivo plasma half-life. Leuprorelin is a linear peptide, a synthetic analogue of gonadotropin-releasing hormone (GnRH), which consists of nine amino acids, containing seven proteinogenic amino acids. It has one D-amino acid (D-leucine), ethyl amidated C-terminus and its N-terminus contains pyroglutamic acid. Due to the modifications, its approximated terminal half-life in vivo in human is 3 h [9]. Cetrorelix is a further modified analogue of GnRH, as of the ten total amino acids, only five are proteinogenic amino acids. It has acetylated N-terminus, amidated C-terminus and the first three constituents of the N-terminus are synthetic amino acids, decreasing the affinity of natural peptidases to the region. Two D-amino acids, D-citrulline and D-alanine, further improve the in vivo stability of cetrorelix, and its in vivo half-life after subcutaneous dosing is around 30 h [10]. Lastly, cyclosporine is a cyclic peptide, consisting of eleven amino acids, of which four are non-proteinogenic amino acids. The non-proteinogenic amino acids are D-alanine, butenyl-methyl-threonine, L-alpha-aminobutyric acid, and sarcosine. Also, seven of the amino acid bonds are N-methylated to improve its stability against hydrolytic enzymes [11]. Its half-life in blood varies between 6 and 20 h [12]. Unlike other peptide therapeutics in this study, its metabolism occurs via CYP3A4, and it is known to metabolize to more than 30 metabolites in vivo [13]. The hepatic metabolism of the aforementioned peptide drugs have been recently reported, and especially the number of metabolites and level of metabolism in the liver S9 fraction can be used as a baseline compared to intestinal and kidney metabolic activity [14]. The stability of the selected peptide drugs were studied in S9 fractions derived from kidney and intestinal tissue, plasma with EDTA or heparin as anticoagulant, and proximal tubule cells. The disappearance and metabolic fate of leuprorelin was further studied in human kidney microsomes and cytosol.

2. Material and methods

2.1. Reagents and materials

HPLC grade methanol was purchased from Merck (Lichrosolv GG, Darmstadt, Germany). HPLC grade acetic acid and ammonium formate were purchased from BDH Laboratory Supplies (Poole, England). Laboratory water was prepared in-house with Direct-Q water purifier (Millipore, Molsheim, France). Human kidney and intestinal S9 fractions, human kidney microsomes and cytosol, in vitro GRO PT media, and human kidney proximal tubule cells were purchased from Bioreclamation IVT (Brussels, Belgium). Plasma (respective anticoagulants K2-EDTA and heparin) was prepared from blood obtained from Finnish Red cross blood service. Nicotinamide adenine dinucleotide phosphate (NADPH), monopotassium phosphate (KH_2PO_4), disodium phosphate (Na_2HPO_4,), penicillin, cyclosporine (purity $\geq$ 98.0%), leuprorelin (European Pharmacopeia reference standard, LEUPRORELIN CRS batch 6, catalogue number L0376000), and cetrorelix (purity >97.5%) were purchased from Sigma-Aldrich (Helsinki, Finland). Phosphate buffer (pH 7.4) was prepared in-house by weighing 2.722 g of KH_2PO_4, 11.35 g of Na_2HPO_4 and 0.476 g of $MgCl_2$ into a container and 1 l of ultra-purified water was added to obtain 100 mM phosphate buffer. pH of the phosphate buffer was adjusted with sodium hydroxide (NaOH).

Stock solutions (10 mM) of leuprorelin and cetrorelix were prepared by weighing calculated amount of peptide into glass vial and diluting by 20% dimethyl sulfoxide (DMSO) in water (v/v). Due to solubility issues, cyclosporine was first diluted by DMSO to obtain 10 mM stock solution; further dilution was obtained by adding 20% DMSO in MeOH (v/v).

2.2. Kidney and intestinal S9 fraction incubations

Both kidney and intestinal S9 fraction incubations were performed similarly. Human S9 fractions (mixed gender pool, kidney lot FBY, intestinal lots SHN and ZJL) were diluted into 100 mM phosphate buffer (pH 7.4) with 2 mM $MgCl_2$ to obtain final protein concentration of 2 mg/ml in the incubation. A 297 μl aliquot of the mixture was preincubated for 6 min at 37 °C in a shaking (600 rpm) incubator block (Eppendorf Thermomixer 5436, Germany) and the reaction was started via addition of 3 μl of study compound (1000 μM in 20% DMSO), to have final test concentrations of 10 μM, with 0.2% DMSO. Assay was performed as a single incubation and analytical injection. The incubations were performed with and without NADPH (1 mM). 40 μl samples were collected at 0 min, 10 min, 20 min, 40 min and 60 min timepoints. The reaction was terminated by adding two-fold volume of ice cold 75% acetonitrile in water (v/v) containing 100 nM phenacetin as an internal standard. Each sample was centrifuged (13 000 g, 10 min at room temperature, Heraeus Pico 17, Thermo Scientific), and the clear supernatant was collected for immediate analysis.

2.3. Plasma incubations

Incubations were performed with K2-EDTA or heparin as anticoagulants. Fresh plasma was prepared from the donated blood by centrifuging it in 1 ml aliquots (1800 g, 10 min at room temperature, Heraeus Pico 17, Thermo Scientific) that resulted into approximately 500 μl plasma recovery. A 490 μl aliquot of the fresh was preincubated for 10 min at 37 °C in a shaking incubator block and the assay was started via addition of 10 μl of study compound (1000 μM and 100 μM in 20% DMSO), to have final test concentrations of 10 and 1 μM, with 0.4% DMSO. The samples of 40 μl were collected at 0 min, 5 min 10 min, 20 min, 40 min, 60 min and 120 min timepoints and the reaction was terminated by adding two-fold volume of ice cold acetonitrile in water (v/v) containing 100 nM phenacetin. Each sample was then centrifuged, and the supernatant was collected for immediate analysis.

2.4. Proximal tubule cells incubations

Vials of cryo-preserved human kidney proximal tubules (lot HVL, one donor) were thawed in water bath and were then suspended into InVitro GRO PT-medium with 1% penicillin and diluted to obtain 100 000 viable proximal tubules per one millimeter cell density, determined by trypan blue exclusion test [15]. 75 μl of resuspended cells were plated on a 96-well plate and the cells were incubated at 37 °C for four hours, after which the medium was replaced with 100 μl of fresh medium. The cells were incubated for two days for them to achieve a monolayer of cells. The metabolic stability assay was performed by preparing InVitro GRO PT-medium with 10 μM of model peptides, respectively, and replacing the thawing medium with 100 μl of the test medium. Samples of 60 μl were collected after 0, 1 h, 2 h, 4 h and 24 h of incubation and immediately terminated with two-fold addition of 75% acetonitrile in water (v/v) containing 100 nM phenacetin as an internal standard. Each sample was centrifuged just before analysis, and the supernatant was collected for analysis.

2.5. Kidney microsomes and cytosol incubations

Leuprorelin metabolism was further studied in human kidney microsomes and cytosol. Human kidney microsomes (mixed gender pool, lot LUN) and cytosol (mixed gender pool, lot NBV) were diluted into 100 mM phosphate buffer (pH 7.4) with 2 mM $MgCl_2$ to obtain a final protein concentration of 1 mg/ml in the incubation. A 297 µl aliquot of the mixture was preincubated for 6 min at 37 °C in a shaking incubator block (Eppendorf Thermomixer 5436, Germany) and the reaction was started via addition of 3 µl of study compound (1000 µM in 20% DMSO), to have final test concentrations of 10 µM, with 0.2% DMSO. Assay was performed as a single incubation and injection. The incubations were performed with and without NADPH (1 mM). 40 µl samples were collected at 0 min, 10 min, 20 min, 40 min and 60 min timepoints. The reaction was terminated by adding two-fold volume of ice cold 75% acetonitrile in water (v/v) containing 100 nM phenacetin as an internal standard. Each sample was centrifuged (13 000 g, 10 min in room temperature, Heraeus Pico 17, Thermo Scientific), and the clear supernatant was collected for immediate analysis.

2.6. Liquid chromatography / high-resolution mass spectrometry

Acquity ultra high pressure liquid chromatography (UPLC) system (Waters Corp, Milford, MA, USA) was used for the experiments. The used analytical column and eluents for the chromatographic separation were peptide dependent. For leuprorelin and cetrorelix, reversed-phase column BEH C18 (2.1×50 mm, 1.7 µm, Waters Corp) with guard filter was used. The used eluents were 0.1% acetic acid in water (v/v, A, pH 3.2) and methanol (B). The gradient elution for leuprorelin and cetrorelix was as follows: 2–2–10–50–95–95 B% in 0–0.5–2–3.5–7–8 min with one minute equilibration in initial conditions. The column oven temperature was 35 °C, injection volume was 4 µl and the flow rate was 0.5 ml/min. The used analytical column for cyclosporine was reversed-phase column BEH Shield RP18 (2.1 ×50 mm, 1.7 µM, Waters Corp) with guard filter and eluents were 2 mM ammonium formate in water (A, pH 6.3) and methanol (B). The gradient elution for cyclosporin was as follows: 2–2–70–95–95 B% in 0–0.5–5–7–8 min with one minute of equilibration in initial conditions. The column oven temperature was 70 °C, injection volume was 4 µl and the flow rate was 0.5 ml/min.

High-resolution mass spectrometry data was acquired with a Thermo Scientific Q-Exactive hybrid quadrupole-orbitrap mass spectrometer (QE-Orbitrap-MS, Thermo Scientific, Waltham, MA, USA). The data acquisition was performed at data-dependent-MS^2 mode which performed a full spectral scan and triggered further MS/MS experiments for ions in inclusion list, and also for the most abundant ions not included in inclusion list. The mass range of m/z 140–2100 was acquired, with acquisition time of 7 Hz, maximum interval time being 100 ms. The used capillary voltage was 3000 V and capillary temperature of 320 °C was used. The auxiliary gas heater temp was set at 500 °C. Nitrogen was used as Auxiliary gas at 20 arbitrary units, Sheath gas at 50 arbitrary units and as a Sweep gas at 5 arbitrary units. External calibration was performed on a weekly basis with Pierce™ LTQ Velos ESI Positive and Negative Ion Calibration Solutions (Thermo Scientific).

2.7. Data analysis

The peptide drugs included in this study and their sequence together with detected LC-HRMS parameters are presented in Table 1. Thermo Xcalibur 4.0 software was used to operate both the mass spectrometer and UPLC-system, and for chromatographic peak integration. The ion chromatograms were extracted from the total ion chromatograms using calculated monoisotopic accurate masses with 5 mDa window. The metabolites were mined from the data using software-aided data processing (Thermo Compound Discoverer 2.1., including structure-intelligent dealkylation tool & mass defect filter, Thermo Scientific) with manual confirmation. The in vitro half-lives in different metabolic systems were extrapolated using the formula $t_{½} = \ln 2/b$, where b is the slope of the linear curve fitted on the natural logarithm on the percentage remaining of the parent compound versus incubation time.

Table 1
List of model peptide drugs.

Name	Sequence	Molecular weight (Da)	m/z	Ion type
Leuprorelin	Pyr1 H2 W3 S4 Y5 L6 L7 R8 P9 NHEt	1209.4	605.3300	$[M+2H]^{2+}$
Cetrorelix	Ac{d-A[3-(2-naphtyl)]}1 [d-F(4-Cl)]2 {d-A[3-(3-pyridyl)]}3 S4 Y5 (D-Cit) 6 L7 R8 P9 d-A10 NH2	1431.0	715.8422	$[M+2H]^{2+}$
Cyclosporine	c{d-A1 L2 L3 V4 Bmt5 Abu6 Sar7 L8 V9 L10 A11}	1202.6	601.9280	$[M+2H]^{2+}$

3. Results and Discussion

The disappearance data was used to derive the half-life and intrinsic clearance, when applicable, of the model peptides. Summary of the observed metabolic turnover and the detected metabolites are collected to Tables 2–6, and the elucidated hydrolytic sites are shown in Figs. 1 and 2. The metabolite numbering was matched with our recent work [14], to ease comparison of the results and metabolite profiles with those hepatic models.

3.1. Leuprorelin

In the NADPH-supplemented incubations with human kidney and intestinal S9 fractions, leuprorelin disappearance was considerably faster in kidney than in intestine, as the half-lives were 9.8 and 51 min, respectively. In the absence of NADPH, the half-lives were 35 min in kidney and 100 min in intestinal S9 fraction, suggesting involvement of metabolism via NADPH dependent enzymes. Leuprorelin was stable in the EDTA and heparin plasma, as well as in the incubations with proximal tubule cells.

In total, 17 metabolites (M1-M17, Table 2) were detected in the incubations with the investigated extrahepatic metabolic systems. In the

Table 2
Half-lives (min) and intrinsic clearances (in parenthesis, µl/min/mg of protein for S9, µl/min/million cells for proximal tubule cells, µl/min/ml for plasma) of each peptide in each metabolic model. HKS9: human kidney S9 fraction, HKM: human kidney microsomes, HKC: human kidney cytosol, HIS9: human intestinal S9 fraction.

	Leuprorelin		Cetrorelix		Cyclosporine	
Enzyme source	T½ (min)	Cl_{int}	T½ (min)	Cl_{int}	T½ (min)	Cl_{int}
HKS9 + NADPH	9.80	35.3	35.2	9.84	192	1.80
HKS9 – NADPH	35.3	9.81	33.8	10.3	149	2.33
HKM + NADPH	260	2.67	-	-	-	-
HKM – NADPH	320	2.20	-	-	-	-
HKC + NADPH	14.0	49.7	-	-	-	-
HKC – NADPH	56.1	12.4	-	-	-	-
Proximal tubule	> 9747	< 0.29	> 9750	< 0.29	1910	1.45
HIS9 + NADPH	51.3	6.75	121	2.87	233	1.49
HIS9 – NADPH	100	3.46	135	2.58	295	1.17
Plasma EDTA	> 790	< 0.88	> 790	< 0.88	> 790	< 0.88
Plasma Heparin	> 790	< 0.88	> 790	< 0.88	> 790	< 0.88

Table 3
Formed metabolites of leuprorelin and their percentual abundances in the end of the incubation in kidney derived models, based on LC/MS peak area compared to parent at 0 min. Order by ascending retention time. The site of hydrolysis in parenthesis. Some metabolites had higher abundance in earlier time points. [1])3.3% at 20 min time point, [2])1.7% at 20 min time point, [3])4.6% at 10 min timepoint, [4]) 10.9% at 40 min timepoint, [5]) 54.4% at 20 min time point and [6]) 1.7% at 20 min timepoint. HKS9: human kidney S9 fraction, HKM: human kidney microsomes, HKC: human kidney cytosol.

	Name	Sequence	HKS9 + NADPH %	HKS9 – NADPH %	HKM + NADPH %	HKM – NADPH %	HKC + NADPH %	HKC – NADPH %	Proximal tubule %
	Leuprorelin	PyrHWSYLLRPNHEt	1.6	31.9	85.4	88.1	5.3	47.5	94.6
M1	2 x hydrolysis (Ser4-Tyr5 + Leu7-Arg8)	YLL	0.4		0.1	0.02			0.1
M2	2 x hydrolysis (His2-Trp3 + Pro9-NHEt)	WSYLLRP	0.6				1.1	0.3	
M3	hydrolysis (Pro9-NHet)	PyrHWSYLLRP	2.8	54.2	8.0	8.9	5.8	41.9	0.9
M4	2 x hydrolysis (His2-Trp3 + Arg8-Pro9)	WSYLLR	0.2				0.1		
M5	2 x hydrolysis (Ser4-Tyr5 + Pro9-NHEt)	YLLRP	35.6	1.9	0.3	0.1	4.9	0.8	0.1
M6	hydrolysis (His2-Trp3)	WSYLLRPNHEt	0.2([1]		0.3	0.1	0.6	0.3	0.1
M7	2 x hydrolysis (Pyr1-His2 + Pro9-NHEt)	HWSYLLRP	0.6([2]				1.0	0.03	
M8	hydrolysis (Pyr1-His2)	HWSYLLRPNHEt	0.2([3]		0.2	0.1	0.5	0.02	
M9	2 x hydrolysis (Trp3-Ser4 + Pro9-NHEt)	SYLLRP	5.1([4]	0.1	0.02		12.6	1.3	
M10	2 x hydrolysis (Tyr5-Leu6 + Pro9-NHEt)	LLRP					3.2	0.3	
M11	hydrolysis (Ser4-Tyr5)	YLLRPNHEt	63.1	3.1	6.8	2.9	18.1	4.0	4.7
M12	hydrolysis (Leu6-Leu7)	LRPNHEt	3.2	0.1	1.3	0.5	9.0	1.5	0.2
M13	hydrolysis (Trp3-Ser4)	SYLLRPNHEt	8.7([5]	0.3([6]	0.9	0.4	34.7	5.7	0.5
M14	hydrolysis (Trp3-Ser4)	PyrHW			0.1	0.1		0.4	0.2
M15	hydrolysis (Arg8-Pro9)	PyrHWSYLLR	0.5	7.9			0.4	3.6	
M16	hydrolysis (Leu7-Arg8)	PyrHWSYLL							0.5
M17	2 x hydrolysis (Ser4-Tyr5 + Arg8-Pro9)	YLLR	3.7	0.1	0.2	0.2			

Table 4
Formed metabolites of leuprorelin and their percentual abundances in the end of the incubation, based on LC/MS peak area compared to parent at 0 min. Order by ascending retention time. The site of hydrolysis in parenthesis. HIS9: human intestinal S9 fraction.

	Name	Sequence	HIS9 + NADPH %	HIS9 – NADPH %	Plasma EDTA %	Plasma Heparin %
	Leuprorelin	PyrHWSYLLRPNHEt	45.2	64.2	102.8	99.2
M3	hydrolysis (Pro9-NHet)	PyrHWSYLLRP	44.5	27.3		
M5	2 x hydrolysis (Ser4-Tyr5 + Pro9-NHEt)	YLLRP	2.5	1.3		
M6	hydrolysis (His2-Trp3)	WSYLLRPNHEt			0.2	
M8	hydrolysis (Pyr1-His2)	HWSYLLRPNHEt				0.1
M11	hydrolysis (Ser4-Tyr5)	YLLRPNHEt	6.9	5.0	0.4	0.2
M12	hydrolysis (Leu6-Leu7)	LRPNHEt				0.1
M13	hydrolysis (Trp3-Ser4)	SYLLRPNHEt	0.3	0.4		0.1
M16	hydrolysis (Leu7-Arg8)	PyrHWSYLL			0.1	0.3

Table 5
Formed metabolites of cetrorelix and their percentual abundances in the end of the incubation, based on LC/MS peak area compared to parent at 0 min. Order by ascending retention time. The site of hydrolysis in parenthesis.

	Name	Sequence	HKS9 + NADPH %	HKS9 – NADPH %	Proximal tubule %	HIS9 + NADPH %	HIS9 – NADPH %	Plasma EDTA %	Plasma Heparin %
	Cetrorelix	Ac{d-A[3-(2-naphtyl)]}[d-F(4-Cl)]{d-A[3-(3-pyridyl)]}SY(D-Cit)LRP{d-A}-NH2	33.2	30.6	100	73.2	75.0	107	99.8
M1	hydrolysis (Leu7-Arg8)	Ac{d-A[3-(2-naphtyl)]}[d-F(4-Cl)]{d-A[3-(3-pyridyl)]}SY(D-Cit)L	0.2	0.1	0.8	2.3	0.5		0.2
M2	hydrolysis (Pro9-D-Ala10)	Ac{d-A[3-(2-naphtyl)]}[d-F(4-Cl)]{d-A[3-(3-pyridyl)]}SY(D-Cit)LRP	5.5	1.5	0.3	15.3	2.3		
M3	hydrolysis (Arg8-Pro9)	Ac{d-A[3-(2-naphtyl)]}[d-F(4-Cl)]{d-A[3-(3-pyridyl)]}SY(D-Cit)LR	8.2	6.0					
M7	hydrolysis (D-Cit6-Leu7)	LRP{d-}-NH2	0.1						
M8	hydrolysis (Tyr5-D-Cit6)	(D-Cit)LRP{d-A}-NH2				0.3	0.3		

incubations with NADPH supplemented kidney S9 fraction, 14 of these were detected, while in the absence of NADPH only eight metabolites were detected, suggesting that metabolism is partly NADPH dependent. In the incubation with kidney S9 fraction in the absence of NADPH, M3 formed via hydrolysis of the N-ethylamide group of the C-terminus was a clear main metabolite. On the contrary, in the presence of NADPH, M5

Table 6
Formed metabolites of cyclosporine and their percentual abundances in the end of the incubation, based on LC/MS peak area compared to parent at 0 min. Order by ascending retention time. The site of hydrolysis in parenthesis. The remaining parent percentage is different from the stability study because higher compound concentration was used.

	Name	Sequence	HKS9 + NADPH %	HKS9 – NADPH %	Proximal tubule %	HIS9 + NADPH %	HIS9 – NADPH %	Plasma EDTA %	Plasma Heparin %
	Cyclosporine	c{D-ALLVBmtAbuSarLVLA}	77.6	68.6	49.5	75.9	84.5	116	99
M6	Oxidation (+O)	c{D-ALLVBmtAbuSarLVLA}			0.2				

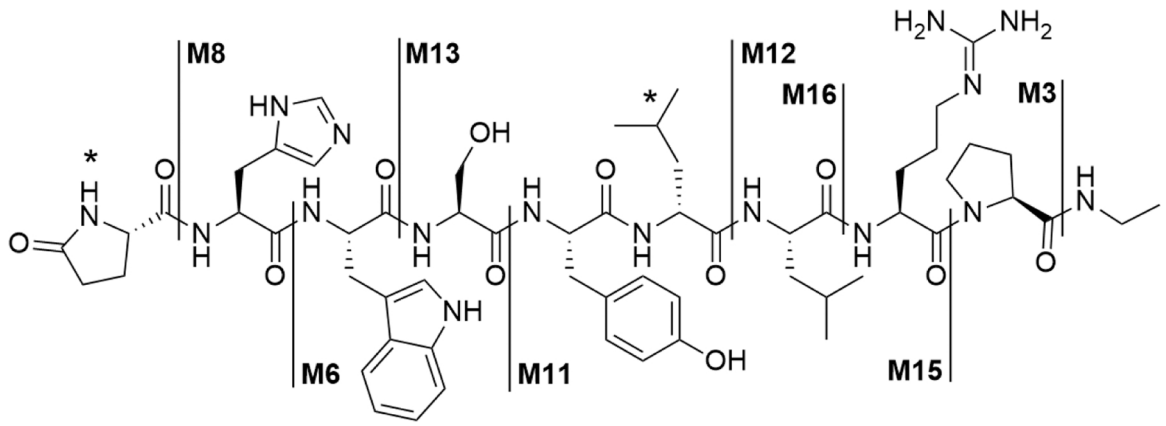

Fig. 1. The hydrolysis sites for the observed hydrolytic cleavage sites for leuprorelin. All other metabolites were formed via same reactions, by their combinations. Asterisks depict the non-proteinogenic amino acids.

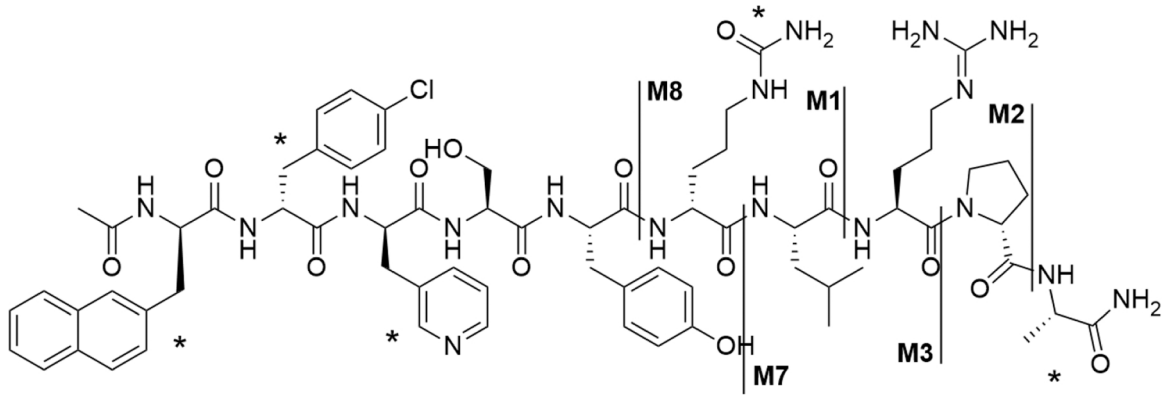

Fig. 2. The hydrolysis sites for the observed hydrolytic cleavage sites for cetrorelix. Asterisks depict the non-proteinogenic amino acids.

and M11 were the clear main metabolites at 60 min time point, as about 88% of the total related LC/MS peak area originated from these metabolites. M11 is formed by a single hydrolytic cleavage between amino acids Ser4 and Tyr5 in highly NADPH dependent manner, and M5 is subsequently hydrolyzed at the C-terminus (the same NADPH independent reaction forming M3, or alternatively M5 formes via M3). M11 is also further metabolized to metabolites M1 and M17, whose formation was NADPH dependent. Thus, based on the data it seems M3 is formed NADPH independently, and then in the presence of NADPH it is metabolized further to form M2, M5, M7 and M9 that were mostly NADPH dependent. The second most abundant metabolite formed in kidney S9 fraction without NADPH was M15, formed by a single hydrolysis between amino acids Arg8 and Pro9 and in addition to M3, M15 was the only metabolite whose formation in kidney S9 fraction was not NADPH dependent. NADPH dependent drug metabolizing enzymes seem to activate the peptide bonds to hydrolyze the more sterically hindered sections. On the contrary to the higher number of metabolites with kidney S9 fraction, only four metabolites were detected in the incubations with intestinal S9 fraction, where M3 was clearly the most abundant metabolite, followed by M11 > M5 > M13, and on the contrary to kidney S9 fraction, no signs of NADPH dependent metabolite formation were observed. Even though no clear disappearance of leuprorelin was observed in the other metabolic systems, some low-level metabolites were still detected. In EDTA plasma M6, M11 and M16 were detected in low abundances, while in heparin plasma M8, M11, M12, M13 and M16 were observed. In the incubation with proximal tubule cells, nine metabolites were detected and again, the main metabolite was M11, followed in abundance by M3, M13 and M16.

In our earlier work with liver S9 fraction, similar NADPH dependency was observed in the formation of leuprorelin metabolites, and involvement of CYP enzymes was speculated [14]. However, due to the similar observation with kidney S9 fraction, in the presence of clearly lower CYP activities, the NADPH effect was further investigated by using incubations with kidney microsomes and cytosol to determine whether

the NADPH dependency was caused by microsomal enzymes (i.e. CYPs or flavin-containing mono-oxygenases (FMOs)[16,17]).

In these experiments the metabolic turnover was clearly limited in microsomes, as 85% of the initial leuprorelin was remaining after 60 min incubation, and no NADPH dependency was detected. On the contrary, a clear NADPH dependent disappearance was observed in kidney cytosol, as the half-life in the presence and absence of NADPH was 14 min vs 56 min, respectively. 11 metabolites were detected in the incubations with human kidney microsomes in the presence NADPH, while 10 were observed in the absence of NADPH. In both experiments, two clear main metabolites were M3 and M11, which indicates that the enzyme responsible for the hydrolysis between serine and tyrosine is active in microsomal fraction of enterocytes. The amount of M3 was similar between the experiments, and about a two-fold higher formation of M11 was detected in the presence of NADPH. Generally, no clear NADPH dependency in metabolite formation was observed in kidney microsomes, although formation of some low-level metabolites were slightly higher in the presence of NADPH. In the incubation with human kidney cytosol, 13 metabolites were detected in the presence and in the absence of NADPH. Similarly to kidney S9 fraction, in the absence of NADPH the clear main kidney cytosol metabolite was M3, with about 42% abundance vs leuprorelin 0 min peak area. Other notable metabolites were M11, M13 and M15 with about 4 – 6% abundances each. All metabolites were a result of single hydrolysis, M3 between the proline and ethylated N-terminus, M11 between serine and tyrosine, M13 between Trp3 and Ser4, and M15 between Arg8 and Pro9. Also similarly to kidney S9 fraction, incubation with the kidney cytosol showed a clear NADPH dependency in metabolite formation, with lower abundance of M3 and M15, and clearly increased formation of all other metabolites, of which M13 and M11 were the most abundant, both formed via single hydrolysis as previously discussed. The next abundant were M9, M12, M5 and M10, of which others than M12 are all formed via M3 by further hydrolysis reactions. M9 is related both to the M3 and M13, as it is the result of two hydrolysis between Pro9 and ethylated C-terminus and Trp3 and Ser4. M5 is formed via enzymes responsible for the hydrolysis of M3 and M11, as after the hydrolysis of Pro9 and C-terminus, it is further hydrolyzed between Ser4 and Tyr5. M10 has the lowest abundance of the M3 related metabolites, and it is formed with additional hydrolysis between tyrosine and leucine.

Thus, the results suggest that NADPH dependency in observed leuprorelin hydrolytic reactions are rather catalyzed by cytosolic enzymes, the NADPH dependency is not caused by CYPs or FMOs, and some further research would be needed to clarify the mechanism of the observed NADPH dependent metabolism. To further speculate on the topic, there are numerous different mechanisms and enzymes, which might cause this [18].

Compared to previously obtained stability data in liver S9 fraction, the disappearance of leuprorelin was quite similar, as the half-lives in the presence NADPH were 12 min in liver S9 fraction and 10 min in kidney S9 fraction, while in the absence of NADPH a half-live of 35 min was obtained, in both liver and kidney S9 fraction. The activity of the enzymes responsible for the metabolism of leuprorelin was thus equivalent between these two systems. In intestinal S9 fraction, the half-life was longer, as the half-life in the presence of NADPH was 51 min and in the absence of NADPH 100 min. The metabolite profiles between liver and kidney S9 fractions were qualitatively similar, although the relative abundances of the metabolites differed, with a higher role of M2, M6, M7 and M8 in liver S9 fraction, while in the kidney S9 fraction M5 and M11 had relatively higher abundances, and M15 and M17 were detected in kidney S9 fraction only. In absence of NADPH in both tissues, the clear main metabolite was M3. For intestinal S9 fraction, NADPH dependency was not detected, and the main metabolite M3 was the same as in the liver and kidney S9 fractions without NADPH. No comprehensive human in vivo metabolism data has been released for leuprorelin [19]. As it is mentioned in Lupron package insert [9] and in an article by Sofianos et al [20]., four metabolites of leuprorelin have been identified in animals and human. The metabolites include pentapeptide M–I (YLLRPNHEt, corresponding to metabolite M11 in this study), tripeptide M–II (YLL, which corresponds to metabolite M1) and tripeptide M–III (PyrHW, corresponding to M14). Dipeptide M–IV (PyrH) was not detected directly in this study, but the corresponding metabolite of hydrolyzed leuprorelin (WSYLLRPNHEt, M6) was detected. Tentative in vitro–in vivo correlation based on this limited data seems to be better in the incubations with human liver and kidney S9 fractions supplemented with NADPH, than in the incubations without NADPH. Yet, M3, the major metabolite in the incubations without NADPH has not been reported to form in vivo. Also, the main metabolites produced in the NADPH supplemented incubations with proximal tubules and kidney S9 fraction were more similar than the main metabolites formed in the incubations with hepatocytes and NADPH supplemented liver S9 fraction [14].

Furthermore, the stability of leuprorelin has been determined earlier as a part of 17 peptide drug study in human gastric and small intestinal fluid, and in simulated gastric and intestinal fluid, by incubating the peptides at 37 °C for two hours [21]. Leuprorelin was shown to degrade rapidly with human intestinal fluids containing pancreatin, but no metabolite formation was reported. The fast degradation of leuprorelin within the intestine [22] is thus most likely a consequence of pancreatic hydrolytic enzymes, and partly explains the slow disappearance in intestinal S9 fraction containing enterocytic hydrolytic enzymes [23]. Guo et al. have studied the transport of leuprorelin through rat and rabbit intestine using everted gut technique, as well as Caco-2 cell monolayers [24]. The apparent permeability was the highest in rat intestine, followed by the permeability in rabbit intestine. In Caco-2 cell culture, consisting of immortalized human epithelial cells, the transport was very limited, with apparent permeability value between 0.45 and 0.56×10^{-6} cm/s. The limited permeability likely explains the high stability of leuprorelin in cell-based models, such as hepatocytes and proximal tubule cells.

3.2. Cetrorelix

For cetrorelix, the disappearance in the human kidney S9 fraction was similar with and without NADPH, with half-lives of about 34 – 35 min. Thus, the disappearance was non-CYP dependent. Also, in human intestinal S9 fraction, disappearance was about similar with and without NADPH, and 4-fold slower than in the kidney S9 fraction, as the half-lives were 121 – 135 min. Cetrorelix was stable in both EDTA and heparin plasma, and in the incubations with proximal tubule cells.

In total, five cetrorelix metabolites (M1 – M3, M7, and M8) were detected in the studied enzymatic systems (Table 3). All metabolites were formed via single cleavage between amino acids. Most abundant metabolites were formed by cleaving amino acids from the unprotected C-terminal of cetrorelix. In incubations with human kidney S9 fraction, the most abundant metabolite was M3 (hydrolysis between Arg8 and Pro9), followed by M2 (cleaving amidated alanine from C-terminal). Two other minor metabolites, M1 and M7, were also detected with kidney S9 fraction. The metabolite profile was similar between the incubations with and without NADPH, although the amount of the detected metabolites was slightly lower in the incubations without NADPH, and low level of M7 was detected only in the presence of NADPH. In the incubations with human intestinal S9 fraction, M1, M2 and M8 were detected, M2 being the most abundant, similarly to earlier liver S9 fraction results [14]. Formation of M1 and M2 was about 5 – fold higher in the presence of NADPH (vs. absence). M3, i.e the main metabolite formed in the human kidney S9 fraction, was not detected at all in the intestinal S9 fraction. Similarly to leuprorelin metabolite M17, which was also formed via hydrolysis between arginine and proline, M3 was detected only with kidney S9 fraction, suggesting that human intestinal S9 fraction might lack peptidases to cleave this bond, while M3 was observed also in liver S9 fraction [14]. Due to the unique structure of proline, the related amide bonds are often resistant to many broad

specific peptidases and many proline specific endo- and exopeptidases have been characterized [25]. No cetrorelix metabolites were detected in EDTA plasma, while M1 was detected in heparinized plasma in low abundance. Two metabolites (M1 and M2) were detected in low abundance in the incubation with proximal tubule cells.

Of the observed cetrorelix metabolites, M1, M2 and M7 have been reported in studies with rat and dogs after subcutaneous dosing by Schwahn et al [26]., who also reported a metabolite formed via hydrolysis between serine and tyrosine, which was not detected here or in our earlier experiments with hepatic models [14].

The stability of cetrorelix in liver S9 fraction and kidney S9 fraction was rather equivalent, as the half-lives in the incubation in the presence of NADPH were 33 and 35 min, respectively. In the absence of NADPH, the half-lives were 42 and 34 min in liver and kidney S9 fraction. In intestinal S9 fraction, the disappearance was clearly slower, as the half-lives with and without NADPH were 3- to 4-fold longer compared to other S9 fractions. The main metabolites were identical between the liver and kidney S9 fractions (M2 and M3), although the relative abundances of the metabolites differed. M2 was clearly more abundant in liver S9 fraction as M3, but the abundance of M2 and M3 were almost equivalent in kidney S9 fraction. In intestinal S9 fraction, M2 was the main metabolite and M3 was not detected. The hydrolytic metabolites detected in this study have been mostly reported in the literature, most notable exception being the M2 (hydrolysis between Arg8 and Pro9) [19]. Non-proteinogenic amino acids clearly protect the N-terminus of cetrorelix, as all detected metabolites were derived via hydrolyzation of the C-terminus containing proteinogenic amino acids. The alanine in C-terminus has been amidated, but that terminus is still highly susceptible for the proteases. The in vivo metabolism of cetrorelix has a good correlation with the results from experiments with all S9 fractions, and the metabolism between liver and kidney S9 fractions is relatively uniform [14].

3.3. Cyclosporine

The disappearance of cyclosporine was slow in both kidney and intestinal S9 fractions with and without NADPH, as all the half-lives were extrapolated to range from 149 min (kidney S9 fraction without NADPH) to 295 min (intestinal S9 fraction without NADPH). Disappearance was not detected in either EDTA or heparinized plasma. In the proximal tubule cells, cyclosporine disappeared to 57% of the initial concentration during 24 h of incubation, corresponding to extrapolated half-life of 1910 min.

In total, only one cyclosporine metabolite was detected, M6 (oxidation) in proximal tubule cell incubations. Thus, no metabolites were detected in the incubations with kidney or intestinal S9 fractions, suggesting that the observed minor disappearance in these models could be caused by low solubility of cyclosporine [27], and the same phenomenon could explain the disappearance observed with proximal tubule cells, as the abundance of observed metabolite M6 was very low. The M6 observed with proximal tubule cells was the most abundant metabolite with liver S9 fraction, also formed NADPH dependently [14]. The limited metabolism of cyclosporine in these models was as expected due to the known CYP-enzyme catalyzed metabolism and low CYP activities in the employed extrahepatic models [17]. Dai et al [28]. have studied cyclosporine in vitro metabolism using human liver and kidney derived microsomes and they identified CYP3A5 being partially responsible on the metabolism of cyclosporine. Three metabolites were detected in the incubation with liver microsomes in the presence of NADPH, but only one was detected in the incubation with kidney microsomes. Based on their results, CYP3A5, and not CYP3A4, is active in kidney, and the oxidation metabolite formed via CYP3A5 is also formed with CYP3A4. In the gut, cyclosporine depletion was not detected when using human intestinal microsomes as an in vitro model [29]. As microsomes have concentrated amount of CYPs, the lack of metabolism in intestinal S9 fraction is expected.

The CYPs 1A1, 1A2, 1B1, 2A6, 2C19, 2D6 and 2E1 are not expressed in human kidney, while data for CYP 2C8, and 2C9 expression are inconclusive [30]. stabilities of leuprorelin and cyclosporine in the colon has been studied by Wang et al [31]., by using in vitro colonic model comprising of mixed faecal inoculum. The stability of the peptide drugs in intestinal S9 fraction in this study followed the same order, as leuprorelin (or leuprolide, as named in the study by Wang et al.) was less stable than cyclosporine. Cyclosporine has a good permeability across Caco2-cells, as the apparent permeability (P_{app}) is 1.51×10^{-6} cm/s from apical to basal (A to B) and 1.51×10^{-6} cm/s from B to A. It is thus also an efflux substrate, as it is a substrate of P-glycoprotein efflux pump [32].

3.4. Discussion

NADPH dependent metabolism was observed for leuprorelin, in kidney (and earlier with liver S9 fraction), but not in intestinal S9 fraction. On the contrary, the formation of its most abundant cetrorelix metabolite M2 in the intestinal S9 fraction was clearly higher in the presence of NADPH. The NADPH dependency of leuprorelin metabolism was further investigated in human kidney microsomes and cytosol, and the data suggested that the NADPH dependency did rather originate from the metabolism by cytosolic than microsomal enzymes, i.e. excluding involvement of CYP or FMO enzymes. M3, formed via hydrolysis of ethyl-amidated C-terminus, was the clear main metabolite in kidney cytosol in the absence NADPH, while its relative abundance in the presence of NADPH or in kidney microsomes ± NADPH was lower. Further metabolism of M3 was limited in the kidney microsomes and also in kidney cytosol in the absence NADPH, while in kidney cytosol with NADPH, M3 was further metabolized to numerous different metabolites. Also, metabolites formed via single hydrolysis of the three first amino acids from N-terminus (Pyr1, His2, and Trp3) were clearly more abundant in kidney cytosol when incubation was supplemented with NADPH. Yet, the data suggests that in the presence of NADPH, the amide bonds between the three first amino acids are more susceptible, reducing the formation of M3. All the first three amino acids have cyclic, nitrogen containing structures, which, in theory, could first undergo oxidative metabolism, possibly causing the activation of amide bond either by removing steric hinderance via cycle opening reaction or otherwise affecting the chemical environment of the amide bond, making it more susceptible to hydrolytic enzymes. Further studies of the involved drug metabolizing enzymes are needed to elucidate the mechanism of this phenomenon. Use of NADPH as a cofactor should be further investigated, regarding the translation of the obtained in vitro results to in vivo metabolite profiles, as the presence of NADPH seems to increase the overall proteolytic activity of generated S9 fractions.

Plasma metabolism of the investigated peptide drugs was very minor, which is likely as the compounds have passed the development process and optimization of this property. As it is well known, plasma contains a lot of peptidases and proteases normally involved in the hydrolyzing metabolism of the peptides, and it is typical to see instability and hydrolysis of peptide drugs in the early stages of preclinical development processes. The investigated compounds were also mostly stable when incubated with proximal tubule cells derived from human kidney. This may be affected by low cell uptake of the compounds, or alternatively lower metabolic/catabolic activities than with kidney S9 fraction that was employed [33].

4. Conclusions

The investigated peptide drugs showcased different stabilities and metabolism, and both the parent peptide disappearance and metabolite formation were variable depending on the employed metabolic system. In general, the peptide drugs were the least stable and produced the highest number of metabolites in kidney S9 fraction, followed by intestinal S9 fraction. The linear peptide leuprorelin was the least stable

peptide in most of the employed metabolic systems, followed by cetrorelix. Cyclosporin was the most stable of the studied therapeutic peptides in extrahepatic systems, which is expected, as its metabolism is CYP-dependent.

Based on these results, sub-cellular S9 fractions are the models producing the highest number of metabolites when investigating peptide drugs, as the cell-based models might suffer from limited uptake. The permeability and structural moieties prone for oxidative metabolism, and use of NADPH in tissue fraction incubations, should be considered when selecting an in vitro model to investigate peptide metabolism.

List and role of funding sources

Admescope Ltd provided funding for the study. All experiments were conducted in the laboratory of Admescope Ltd and authors designed and conducted the study.

Credit authorship contribution statement

Juha Jyrkäs: Writing – original draft, Study design, Experimental work, Data interpretation. **Ari Tolonen:** Writing – review & editing, Study design, Data interpretation, Resources, Supervision. **Toni Lassila:** Writing – review & editing, Experimental work, Data interpretation.

Declaration of Competing Interest

The authors declare that they have no known competing financial interests or personal relationships that could have appeared to influence the work reported in this paper.

References

[1] A.K. Sato, M. Viswanathan, R.B. Kent, C.R. Wood, Therapeutic peptides: technological advances driving peptides into development, Curr. Opin. Biotechnol. 17 (2006) 638–642, https://doi.org/10.1016/j.copbio.2006.10.002.
[2] K. Fosgerau, T. Hoffmann, Peptide therapeutics: Current status and future directions, Drug Discov. Today 20 (2015) 122–128, https://doi.org/10.1016/j.drudis.2014.10.003.
[3] D.J. Craik, D.P. Fairlie, S. Liras, D. Price, The Future of Peptide-based Drugs, Chem. Biol. Drug Des. 81 (2013) 136–147, https://doi.org/10.1111/cbdd.12055.
[4] S. Maher, D.J. Brayden, Overcoming poor permeability: translating permeation enhancers for oral peptide delivery, Drug Discov. Today Technol. 9 (2012) e113–e119, https://doi.org/10.1016/j.ddtec.2011.11.006.
[5] L. Di, Strategic Approaches to Optimizing Peptide ADME Properties, AAPS J. 17 (2015) 134–143, https://doi.org/10.1208/s12248-014-9687-3.
[6] A. Sonesson, I. Bjørnsdottir, J.K. Christensen, Meeting report: 3rd workshop of the peptide ADME discussion group, Xenobiotica 51 (2021) 1470–1474, https://doi.org/10.1080/00498254.2021.2020377.
[7] R. Böttger, R. Hoffmann, D. Knappe, Differential stability of therapeutic peptides with different proteolytic cleavage sites in blood, plasma and serum, PLoS One 12 (2017), e0178943.
[8] A. Bernkop-Schnürch, T. Schmitz, Presystemic Metabolism of Orally Administered Peptide Drugs and Strategies to Overcome It, 2007.
[9] Lupron package insert, (2014). ⟨https://www.accessdata.fda.gov/%0Adrugsatfda_docs/label/2014/020517s036_019732s041lbl.pdf⟩.
[10] Cetroride package insert, (2019). ⟨https://www.ema.europa.eu/en/documents/product-information/cetrotide-epar-product-information_en.pdf⟩.
[11] J. Dittmann, R.M. Wenger, H. Kleinkauf, A. Lawens, Mechanism of Cyclosporin A Biosynthesis, J. Biol. Chem. 269 (1994) 2841–2846, https://doi.org/10.1016/S0021-9258(17)42019-9.
[12] R.J. Ptachinski, G.J. Venkataramanan, Raman Burckart, Clinical Pharmacokinetics of Cyclosporin, Clin. Pharm. 11 (1986) 107–132, https://doi.org/10.2165/00003088-199529060-00003.
[13] T. Kronbach, V. Fischer, U.A. Meyer, Cyclosporin metabolism in human liver: Identification of a cytochrome P450III gene family as the major cyclosporine-metabolizing enzyme explains interactions of cyclosporine with other drugs, Clin. Pharmacol. Ther. 43 (1988) 630–635.
[14] J. Jyrkäs, A. Tolonen, Hepatic in vitro metabolism of peptides; Comparison of human liver S9, hepatocytes and Upcyte hepatocytes with cyclosporine A, leuprorelin, desmopressin and cetrorelix as model compounds, J. Pharm. Biomed. Anal. 196 (2021), 113921, https://doi.org/10.1016/j.jpba.2021.113921.
[15] W. Strober, Trypan Blue Exclusion Test of Cell Viability, Curr. Protoc. Immunol. 111 (2001) 1–3, https://doi.org/10.1002/0471142735.ima03bs111.
[16] J.R. Cashman, J. Zhang, Human Flavin-Containing Monooxygenases, Annu. Rev. Pharmacol. Toxicol. 46 (2006) 65–100, https://doi.org/10.1146/annurev.pharmtox.46.120604.141043.
[17] O. Pelkonen, M. Turpeinen, J. Hakkola, P. Honkakoski, J. Hukkanen, H. Raunio, Inhibition and induction of human cytochrome P450 enzymes: Current status, Arch. Toxicol. 82 (2008) 667–715, https://doi.org/10.1007/s00204-008-0332-8.
[18] S. Mahesh, K.C. Tang, M. Raj, Amide bond activation of biological molecules, Molecules 23 (2018), https://doi.org/10.3390/molecules23102615.
[19] C.S. Brian Chia, A Review on the Metabolism of 25 Peptide Drugs, Int. J. Pept. Res. Ther. 27 (2021) 1397–1418, https://doi.org/10.1007/s10989-021-10177-0.
[20] Z. Sofianos, T. Katsila, N. Kostomitsopoulos, V. Balafas, J. Matsoukas, T. Tselios, C. Tamvakopoulos, In vivo evaluation and in vitro metabolism of leuprolide in mice - mass spectrometry-based biomarker measurement for efficacy and toxicity, J. Mass Spectrom. 43 (2008) 1381–1392, https://doi.org/10.1002/jms.
[21] J. Wang, V. Yadav, A.L. Smart, S. Tajiri, A.W. Basit, Toward oral delivery of biopharmaceuticals: An assessment of the gastrointestinal stability of 17 peptide drugs, Mol. Pharm. 12 (2015) 966–973, https://doi.org/10.1021/mp500809f.
[22] G. Imanidis, K.C. Hartner, N.A. Mazer, Intestinal permeation and metabolism of a model peptide (leuprolide) and mechanisms of permeation enhancement by non-ionic surfactants, Int. J. Pharm. 120 (1995) 41–50, https://doi.org/10.1016/0378-5173(94)00407-V.
[23] P. Langguth, V. Bohner, J. Heizmann, H.P. Merkle, S. Wolffram, G.L. Amidon, S. Yamashita, The challenge of proteolysis enzymes in intestinal peptide delivery, J. Control. Release 46 (1997) 39–57, https://doi.org/10.1016/S0168-3659(96)01586-6.
[24] J. Guo, Q. Ping, G. Jiang, J. Dong, S. Qi, L. Feng, Z. Li, C. Li, Transport of leuprolide across rat intestine, rabbit intestine and Caco-2 cell monolayer, Int. J. Pharm. 278 (2004) 415–422, https://doi.org/10.1016/j.ijpharm.2004.03.031.
[25] R. Walter, W.H. Simmons, T. Yoshimoto, Proline specific endo- and exopeptidases, Mol. Cell. Biochem. 30 (1980) 111–127, https://doi.org/10.1007/BF00227927.
[26] M. Schwahn, H. Schupke, A. Gasparic, D. Krone, G. Peter, R. Hempel, T. Kronbach, M. Locher, W. Jahn, J. Engel, Disposition and metabolism of cetrorelix, a potent luteinizing hormone- releasing hormone antagonist, in rats and dogs, Drug Metab. Dispos. 28 (2000) 10–20.
[27] P. Berton, M.K. Mishra, H. Choudhary, A.S. Myerson, R.D. Rogers, Solubility Studies of Cyclosporine Using Ionic Liquids, ACS Omega 4 (2019) 7938–7943, https://doi.org/10.1021/acsomega.9b00603.
[28] Y. Dai, K. Iwanaga, Y.S. Lin, M.F. Hebert, C.L. Davis, W. Huang, E.D. Kharasch, K. E. Thummel, In vitro metabolism of cyclosporine A by human kidney CYP3A5, Biochem. Pharmacol. 68 (2004) 1889–1902, https://doi.org/10.1016/j.bcp.2004.07.012.
[29] R.D. Whalen, P.N.V. Tata, G.J. Burckart, R. Venkataramanan, Species differences in the hepatic and intestinal metabolism of cyclosporine, Xenobiotica 29 (1999) 3–9, https://doi.org/10.1080/004982599238777.
[30] K.M. Knights, A. Rowland, J.O. Miners, K. Knights, Renal drug metabolism in humans: the potential for drug-endobiotic interactions involving cytochrome P450 (CYP) and UDP-glucuronosyltransferase (UGT), (2013). https://doi.org/10.1111/bcp.12086.
[31] J. Wang, V. Yadav, A.L. Smart, S. Tajiri, A.W. Basit, Stability of peptide drugs in the colon, Eur. J. Pharm. Sci. 78 (2015) 31–36, https://doi.org/10.1016/j.ejps.2015.06.018.
[32] K.M. Corbett, L. Ford, D.B. Warren, C.W. Pouton, D.K. Chalmers, Cyclosporin Structure and Permeability: From A to Z and beyond, J. Med. Chem. 64 (2021) 13131–13151, https://doi.org/10.1021/acs.jmedchem.1c00580.
[33] A. Komin, L.M. Russell, K.A. Hristova, P.C. Searson, Peptide-based strategies for enhanced cell uptake, transcellular transport, and circulation: Mechanisms and challenges, Adv. Drug Deliv. Rev. 110– 111 (2017) 52–64, https://doi.org/10.1016/j.addr.2016.06.002.